

***CoprolD* predicts the source of coprolites and paleofeces using microbiome composition and host DNA content**

Maxime Borry¹, Bryan Cordova¹, Angela Perri^{2, 11}, Marsha C. Wibowo^{17, 18, 3}, Tanvi Honap^{8, 16}, Wing Tung Jada Ko⁴, Jie Yu⁵, Kate Britton^{11, 15}, Linus Girdland Flink^{15, 19}, Robert C. Power^{11, 12}, Ingelise Stuijts¹³, Domingo Salazar Garcia¹⁴, Courtney A. Hofman^{8, 16}, Richard W. Hagan¹, Thérèse Samdapawindé Kagone⁶, Nicolas Meda⁶, Hélène Carabin⁷, David Jacobson^{8, 16}, Karl Reinhard⁹, Cecil M. Lewis, Jr.^{8, 16}, Aleksandar Kostic^{17, 18, 3}, Choongwon Jeong^{1, 20}, Alexander Herbig¹, Alexander Hübner¹, and Christina Warinner^{1, 4, 10}

¹Department of Archaeogenetics, Max Planck Institute for the Science of Human History, Jena, Germany 07745

²Department of Archaeology, Durham University, Durham, UK DH13LE

³Harvard Medical School, Department of Microbiology, Boston, MA, USA 02215

⁴Department of Anthropology, Harvard University, Cambridge, MA, USA 02138

⁵Department of History, Wuhan University, Wuhan, China

⁶Centre MURAZ, Bobo-Dioulasso, Burkina Faso

⁷Département de pathologie et de microbiologie, Faculté de Médecine vétérinaire-Université de Montréal, Saint-Hyacinthe, Canada, QC J2S 2M2

⁸Department of Anthropology, University of Oklahoma, Norman, OK, USA 73019

⁹School of Natural Resources, University of Nebraska, Lincoln, NE, USA 68583

¹⁰Faculty of Biological Sciences, Friedrich-Schiller University, Jena, Germany, 07743

¹¹Department of Human Evolution, Max Planck Institute for Evolutionary Anthropology, Leipzig, Germany

¹²Institut für Vor- und Frühgeschichtliche Archäologie und Provinzialrömische Archäologie, Ludwig-Maximilians-Universität München, Munich

¹³The Discovery Programme, 6 Mount Street Lower, Dublin 2, Ireland

¹⁴Grupo de Investigación en Prehistoria IT-1223-19 (UPV-EHU)/IKERBASQUE-Basque Foundation for Science (Vitoria, Spain)

¹⁵Department of Archaeology, University of Aberdeen, St Mary's Building, Elphinstone Road, Aberdeen, AB24 3UF, UK

¹⁶Laboratories of Molecular Anthropology and Microbiome Research (LMAMR), University of Oklahoma, Norman, OK, USA 73019

¹⁷Joslin Diabetes Center, Section on Pathophysiology and Molecular Pharmacology, Boston, MA, USA

¹⁸Joslin Diabetes Center, Section on Islet Cell and Regenerative Biology, Boston, MA, USA

¹⁹School of Natural Sciences and Psychology, Liverpool John Moores University, L3 3AF Liverpool, United Kingdom

²⁰School of Biological Sciences, Seoul National University, Seoul, South Korea

Corresponding author:

Maxime Borry, Christina Warinner

Email address: borry@shh.mpg.de, warinner@shh.mpg.de

ABSTRACT

46 Shotgun metagenomics applied to archaeological feces (paleofeces) can bring new insights into the
47 composition and functions of human and animal gut microbiota from the past. However, paleofeces often
48 undergo physical distortions in archaeological sediments, making their source species difficult to identify
49 on the basis of fecal morphology or microscopic features alone. Here we present a reproducible and
50 scalable pipeline using both host and microbial DNA to infer the host source of fecal material. We apply
51 this pipeline to newly sequenced archaeological specimens and show that we are able to distinguish
52 morphologically similar human and canine paleofeces, as well as non-fecal sediments, from a range of
53 archaeological contexts.

54 INTRODUCTION

55 The gut microbiome, located in the distal colon and primarily studied through the analysis of feces,
56 is the largest and arguably most influential microbial community within the body (Huttenhower et al.,
57 2012). Recent investigations of the human microbiome have revealed that it plays diverse roles in
58 health and disease, and gut microbiome composition has been linked to a variety of human health states,
59 including inflammatory bowel diseases, diabetes, and obesity (Kho and Lal, 2018). To investigate the gut
60 microbiome, metagenomic sequencing is typically used to reveal both the taxonomic composition (i.e.,
61 which bacteria are there) and the functions the microbes are capable of performing (i.e., their potential
62 metabolic activities) (Sharpton, 2014). Given the importance of the gut microbiome in human health, there
63 is great interest in understanding its recent evolutionary and ecological history (Warinner and Lewis Jr,
64 2015; Davenport et al., 2017).

65 Paleofeces, either in an organic or partially mineralized (coprolite) state, present a unique opportunity
66 to directly investigate changes in the structure and function of the gut microbiome through time (Warinner
67 et al., 2015). Paleofeces are found in a wide variety of archaeological contexts around the world and are
68 generally associated with localized processes of desiccation, freezing, or mineralization. Paleofeces can
69 range in size from whole, intact fecal pieces (Jiménez et al., 2012) to millimeter-sized sediment inclusions
70 identifiable by their high phosphate and fecal sterol content (Sistiaga et al., 2014). Although genetic
71 approaches have long been used to investigate dietary DNA found within human (Gilbert et al., 2008;
72 Poinar et al., 2001) and animal (Poinar et al., 1998; Hofreiter et al., 2000; Bon et al., 2012; Wood et al.,
73 2016) paleofeces, it is only recently that improvements in metagenomic sequencing and bioinformatics
74 have enabled detailed characterization of their microbial communities (Tito et al., 2008, 2012; Warinner
75 et al., 2017).

76 However, before evolutionary studies of the gut microbiome can be conducted, it is first necessary
77 to confirm the host source of the paleofeces under study. Feces can be difficult to taxonomically assign
78 by morphology alone (Supplementary Note), and human and canine feces can be particularly difficult to
79 distinguish in archaeological contexts (Poinar et al., 2009). Since their initial domestication more than
80 12,000 years ago (Frantz et al., 2016), dogs have often lived in close association with humans, and it is not
81 uncommon for human and dog feces to co-occur at archaeological sites. Moreover, dogs often consume
82 diets similar to humans because of provisioning or refuse scavenging (Guiry, 2012), making their feces
83 difficult to distinguish based on dietary contents. Even well-preserved fecal material degrades over time,
84 changing in size, shape, and color (Figure 1). The combined analysis of host and microbial ancient DNA
85 (aDNA) within paleofeces presents a potential solution to this problem.

86 Previously, paleofeces host source has been genetically inferred on the basis of PCR-amplified
87 mitochondrial DNA sequences alone (Hofreiter et al., 2000); however, this is problematic in the case of
88 dogs, which, in addition to being pets and working animals, were also eaten by many ancient cultures
89 (Clutton-Brock and Hammond, 1994; Rosenswig, 2007; Kirch and O'Day, 2003; Podberscek, 2009), and
90 thus trace amounts of dog DNA may be expected to be present in the feces of humans consuming dogs.
91 Additionally, dogs often scavenge on human refuse, including human excrement (Butler and Du Toit,
92 2002), and thus ancient dog feces could also contain trace amounts of human DNA, which could be
93 further inflated by PCR-based methods.

94 A metagenomics approach overcomes these issues by allowing a quantitative assessment of eukaryotic
95 DNA at a genome-wide scale, including the identification and removal of modern human contaminant

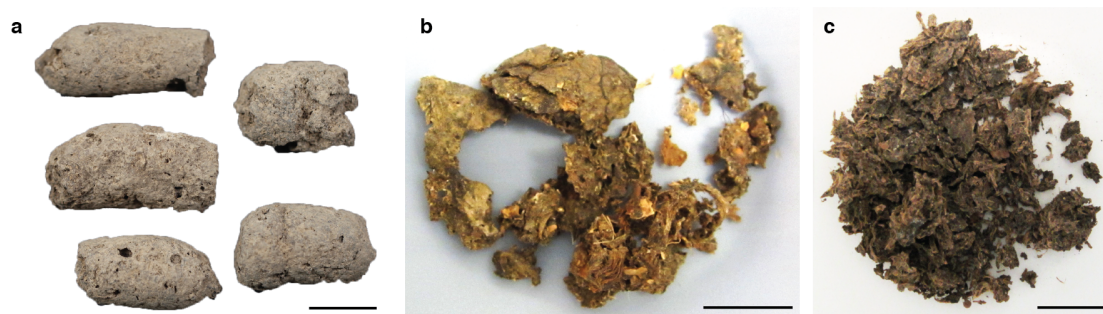


Figure 1. Examples of archaeological paleofeces analyzed in this study.

(a) H29-3, from Anhui Province, China, Neolithic period; (b) Zape 2, from Durango, Mexico, ca. 1300 BP; (c) Zape 28, from Durango, Mexico, ca. 1300 BP. Paleofeces ranged from slightly mineralized intact pieces (a) to more fragmentary organic states (b, c), and color ranged from pale gray (a) to dark brown (c). Each scale bar represents 2 cm.

96 DNA that could potentially arise during excavation or subsequent curation or storage. It also allows for the
97 microbial composition of the feces to be taken into account. Gut microbiome composition differs among
98 mammal species (Ley et al., 2008), and thus paleofeces microbial composition could be used to confirm and
99 authenticate host assignment. Available microbial tools, such as SourceTracker (Knights et al., 2011) and
100 FEAST (Shenhav et al., 2019), can be used to perform the source prediction of microbiome samples from
101 uncertain sources (sinks) using a reference dataset of source-labeled microbiome samples and, respectively,
102 Gibbs sampling or an Expectation-Maximization algorithm. However, although SourceTracker has been
103 widely used for modern microbiome studies and has even been applied to ancient gut microbiome data
104 (Tito et al., 2012) (Hagan et al., 2019), it was not designed to be a host species identification tool for
105 ancient microbiomes.

106 In this work we present a bioinformatics method to infer and authenticate the host source of paleofeces
107 from shotgun metagenomic DNA sequencing data: coproID (**coprolite IDentification**). coproID combines
108 the analysis of putative host ancient DNA with a machine learning prediction of the feces source based
109 on microbiome taxonomic composition. Ultimately, coproID predicts the host source of a paleofeces
110 specimen from the shotgun metagenomic data derived from it. We apply coproID to previously published
111 modern fecal datasets and show that it can be used to reliably predict their host. We then apply coproID to
112 a set of newly sequenced paleofeces specimens and non-fecal archaeological sediments and show that
113 it can discriminate between feces of human and canine origin, as well as between fecal and non-fecal
114 samples.

115 MATERIAL AND METHODS

116 Gut microbiome reference datasets

117 Previously published modern reference microbiomes were chosen to represent the diversity of potential pa-
118 leofeces sources and their possible contaminants, namely human fecal microbiomes from Non-Westernized
119 Human/Rural (NWHR), and Westernized Human/Urban (WHU) communities, dog fecal microbiomes,
120 and soil samples (Table 1). Because the human datasets had been filtered to remove human genetic
121 sequences prior to database deposition, we additionally generated new sequencing data from 118 fecal
122 specimens from both NWHR and WHU populations (Table S5) in order to determine the average propor-
123 tion and variance of host DNA in human feces. The Joslin Diabetes Center granted Ethical approval to
124 sample the WHU individuals. The Centre MURAZ Research Institute granted Ethical approval to sample
125 the NWHR individuals.

Metagenome source	Food production	N	Analysis	Source
Homo sapiens - USA	WHU	36	microbiome	The Human Microbiome Project Consortium et al. (2012)
Homo sapiens - India (Bhopal and Kerala)	WHU & NWHR	19	microbiome	Dhakan et al. (2019)
Homo sapiens - Fiji (agrarian villages)	NWHR	20	microbiome	Brito et al. (2019)
Homo sapiens - Madagascar	NWHR	110	microbiome	Pasolli et al. (2019)
Homo sapiens - Brazil (Yanomami)	NWHR	3	microbiome	Pasolli et al. (2019)
Homo sapiens - Peru (Tunapuco)	NWHR	12	microbiome	Obregon-Tito et al. (2015)
Homo sapiens - Tanzania (Hadza)	NWHR	38	microbiome	Rampelli et al. (2015)
Homo sapiens - Peru (Matses)	NWHR	24	microbiome	Obregon-Tito et al. (2015)
Homo sapiens - USA (Boston)	WHU	49	host DNA	This study
Homo sapiens - Burkina Faso	NWHR	69	host DNA	This study
Canis familiaris	-	150	microbiome and host DNA	Coelho et al. (2018)
Soil	-	16	microbiome	Fierer et al. (2012)
Soil	-	2	microbiome	CSJR and aromatic plants (2016)
Soil	-	2	microbiome	Orellana et al. (2018)

Table 1. Modern reference microbiome datasets

126 **Archaeological samples**

127 A total of 20 archaeological samples, originating from 10 sites and spanning periods from 7200 BP to the
128 medieval era, were selected for this study. Among these 20 samples, of which 17 are newly sequenced, 13
129 are paleofeces, 4 are midden sediments, and 3 are sediments obtained from human pelvic bone surfaces.
130 (Table 2).

Archeological ID	Laboratory ID	Site Name	Region	Period	Sample type	Archaeologically suspected species	Plot ID
Zape 2*	ZSM002	Cueva de los Muertos Chiquitos	Mexico	1300 BP	Paleofeces	HUMAN	01
Zape 5*	ZSM005	Cueva de los Muertos Chiquitos	Mexico	1300 BP	Paleofeces	HUMAN	02
Zape 23	ZSM023	Cueva de los Muertos Chiquitos	Mexico	1300 BP	Paleofeces	HUMAN or CANID	03
Zape 25	ZSM025	Cueva de los Muertos Chiquitos	Mexico	1300 BP	Paleofeces	HUMAN	04
Zape 27	ZSM027	Cueva de los Muertos Chiquitos	Mexico	1300 BP	Paleofeces	HUMAN	05
Zape 28*	ZSM028	Cueva de los Muertos Chiquitos	Mexico	1300 BP	Paleofeces	HUMAN	06
Zape 29	ZSM029	Cueva de los Muertos Chiquitos	Mexico	1300 BP	Paleofeces	HUMAN	07
Zape 31	ZSM031	Cueva de los Muertos Chiquitos	Mexico	1300 BP	Paleofeces	HUMAN	08
H29-1	AHP001	Xiaosungang	China	Neolithic 7200-6800 BP	Paleofeces	CANID or CERVID	09
H35-1	AHP002	Xiaosungang	China	Neolithic 7200-6800 BP	Paleofeces	CANID or CERVID	10
H29-2	AHP003	Xiaosungang	China	Neolithic 7200-6800 BP	Paleofeces	CANID or CERVID	11
H29-3	AHP004	Xiaosungang	China	Neolithic 7200-6800 BP	Paleofeces	CANID or CERVID	12
LG 4560.69	YRK001	Surrey	UK	Post-Medieval	Paleofeces	HUMAN	13
AP3-C197S163	DRL001.A	Derragh	Ireland	Mesolithic	Midden Sediment	-	14
AP4-A6-2860	CBA001.A	Cabeço das Amoreiras	Portugal	Mesolithic	Midden Sediment	-	15
AP5-798-162	BRF001.A	Binchester Roman Fort	England	Roman	Midden Sediment	-	16
AP6-LPZ702	LEI010.A	Leipzig	Germany	10th- 11th century AD	Midden Sediment	-	17
AP7-6-28353	ECO004.D	El Collado	Spain	Mesolithic	Pelvic Sediment	-	18
AP8-CMIN-M1	CMN001.D	Cingle del Mas Nou	Spain	Mesolithic	Pelvic Sediment	-	19
AP9-17590	MLP001.A	Molpir	Slovakia	7th century BC	Pelvic Sediment	-	20

*Metagenomic data were previously published in (Hagan et al., 2019)

Table 2. Archaeological samples

131 **Sampling**

132 Paleofeces specimens from Mexico were sampled in a dedicated aDNA cleanroom in the Laboratories
133 for Molecular Anthropology and Microbiome Research (LMAMR) at the University of Oklahoma, USA.
134 Specimens from China were sampled in a dedicated aDNA cleanroom at the Max Planck Institute for
135 the Science of Human History (MPI-SHH) in Jena, Germany. All other specimens were first sampled at
136 the Max Planck Institute for Evolutionary Anthropology (MPI-EVA) in Leipzig, Germany before being
137 transferred to the MPI-SHH for further processing. Sampling was performed using a sterile stainless
138 steel spatula or scalpel, followed by homogenization in a mortar and pestle, if necessary. Because the
139 specimens from Xiaosungang, China were very hard and dense, a rotary drill was used to section the
140 coprolite prior to sampling. Where possible, fecal material was sampled from the interior of the specimen
141 rather than the surface. Specimens from Molphir and Leipzig were received suspended in a buffer of
142 trisodium phosphate, glycerol, and formyl following screening for parasite eggs using optical microscopy.
143 For each paleofeces specimen, a total of 50-200 mg was analyzed.

144 Modern feces were obtained under written informed consent from Boston, USA (WHU) from a
145 long-term (>50 years) type 1 diabetes cohort, and from villages in Burkina Faso (NWHR) as part of
146 broader studies on human gut microbiome biodiversity and health-associated microbial communities.
147 Feces were collected fresh and stored frozen until analysis. A total of 250 mg was analyzed for each fecal
148 specimen.

149 **DNA Extraction**

150 For paleofeces and sediment samples, DNA extractions were performed using a silica spin column
151 protocol (Dabney et al., 2013) with minor modifications in dedicated aDNA cleanrooms located at
152 LMAMR (Mexican paleofeces) and the MPI-SHH (all other paleofeces). At LMAMR, the modifications
153 followed those of protocol D described in (Hagan et al., 2019). DNA extractions at the MPI-SHH
154 were similar, but omitted the initial bead-beating step, and a single silica column was used per sample
155 instead of two. Additionally, to reduce centrifugation errors, DNA extractions performed at the MPI-SHH
156 substituted the column apparatus from the High Pure Viral Nucleic Acid Large Volume Kit (Roche,
157 Switzerland) in place of the custom assembled Zymo-reservoirs coupled to MinElute (Qiagen) columns
158 described in (Dabney et al., 2013). Samples processed at the MPI-SHH were also partially treated with
159 uracil-DNA-glycosylase (UDG) enzyme to confine DNA damage to the ends of the DNA molecules
160 (Rohland et al., 2015).

161 For modern feces, DNA was extracted from Burkina Faso fecal samples using the AllPrep PowerViral
162 DNA/RNA Qiagen kit at Centre MURAZ Research Institute in Burkina Faso. DNA was extracted from
163 the Boston fecal material using the ZymoBIOMICS DNA Miniprep Kit (D4303) at the Joslin Diabetes
164 Center.

165 **Library preparation and Sequencing**

166 For paleofeces and sediment samples, double-stranded, dual-indexed shotgun Illumina libraries were
167 constructed following (Meyer and Kircher, 2010) using either the NEBNext DNA Library Prep Master Set
168 (E6070) kit (Hagan et al., 2019; Mann et al., 2018) for the Mexican paleofeces or individually purchased
169 reagents (Mann et al., 2018) for all other samples. Following library amplification using Phusion HotStart
170 II (Mexican paleofeces) or Agilent Pfu Turbo Cx Hotstart (all other paleofeces) polymerase, the libraries
171 were purified using a Qiagen MinElute PCR Purification kit and quantified using either a BioAnalyzer
172 2100 with High Sensitivity DNA reagents or an Agilent Tape Station D1000 Screen Tape kit. The Mexican
173 libraries were pooled in equimolar amounts and sequenced on an Illumina HiSeq 2000 using 2x100
174 bp paired-end sequencing. All other libraries were pooled in equimolar amounts and sequenced on an
175 Illumina HiSeq 4000 using 2x75 bp paired-end sequencing.

176 For modern NWHR feces, double-stranded, dual-indexed shotgun Illumina libraries were constructed
177 in a dedicated modern DNA facility at LMAMR. Briefly, after DNA quantification using a Qubit dsDNA
178 Broad Range Assay Kit, DNA was sheared using a QSonica Q800R in 1.5mL 4°C cold water at 50%
179 amplitude for 12 minutes to aim for a fragment size between 400 and 600 bp. Fragments shorter than
180 150 bp were removed using Sera-Mag SpeedBeads and a Alpaqua 96S Super Magnet Plate. End-repair
181 and A-tailing was performed using the Kapa HyperPrep EndRepair and A-Tailing Kit, and Illumina
182 sequencing adapters were added. After library quantification, libraries were dual-indexed in an indexing
183 PCR over four replicates, pooled, and purified using the SpeedBeads. Libraries were quantified using
184 the Agilent Fragment Analyzer, pooled in equimolar ratios, and size-selected using the Pippin Prep to

185 a target size range of 400-600 bp. Libraries were sequenced on an Illumina NovaSeq S1 using 2x150
186 bp paired-end sequencing at the Oklahoma Medical Research Foundation Next-Generation Sequencing
187 Core facility. Modern WHU libraries were generated using the NEBNext DNA library preparation kit
188 following manufacturer's recommendations, after fragmentation by shearing for a target fragment size of
189 350 bp. The libraries were then pooled and sequenced by Novogene on a NovaSeq S4 using 2x150 bp
190 paired-end sequencing.

191 **Proportion of host DNA in gut microbiome**

192 Because it is standard practice to remove human DNA sequences from metagenomics DNA sequence files
193 before data deposition into public repositories, we were unable to infer the proportion of human DNA
194 in human feces from publicly available data. To overcome this problem, we measured the proportion
195 of human DNA in two newly generated fecal metagenomics datasets from Burkina Faso (NWHF) and
196 Boston, U.S.A. (WHU) (Table S5). To measure the proportion of human DNA in each fecal dataset,
197 we used the Anonymap pipeline (Borry, 2019a) to perform a mapping with Bowtie 2 (Langmead and
198 Salzberg, 2012) with the parameters `--very-sensitive -N 1` after adapter cleaning and reads
199 trimming for ambiguous and low-quality bases with a QScore below 20 by AdapterRemoval v2 (Schubert
200 et al., 2016). To preserve the anonymity of the donors, the sequences of mapped reads were then replaced
201 by Ns thus anonymizing the alignment files. We obtained the proportion of host DNA per sample by
202 dividing the number of mapped reads by the total number of reads in the sample. The proportion of host
203 DNA in dog feces was determined from the published dataset Coelho et al. (2018) as described above, but
204 without the anonymization step.

205 **coproID pipeline**

206 Data were processed using the coproID pipeline v1.0 (Figure 2) (DOI: 10.5281/zenodo.2653757) written
207 using Nextflow (Di Tommaso et al., 2017) and made available through nf-core (Ewels et al., 2019).
208 Nextflow is a Domain Specific Language designed to ensure reproducibility and scalability for scientific
209 pipelines, and nf-core is a community-developed set of guidelines and tools to promote standardization
210 and maximum usability of Nextflow pipelines.

211 coproID consists of 5 different steps:

212 **Preprocessing**

213 *Fastq* sequencing files are given as an input. After quality control analysis with FastQC (Andrews et al.,
214 2010), raw sequencing reads are cleaned from sequencing adapters and trimmed from ambiguous and
215 low-quality bases with a QScore below 20, while reads shorter than 30 base pairs are discarded using
216 AdapterRemoval v2. By default, paired-end reads are merged on overlapping base pairs.

217 **Mapping**

218 The preprocessed reads are then aligned to each of the target species genomes (source species) by Bowtie2
219 with the `--very-sensitive` preset while allowing for a mismatch in the seed search (`-N 1`).

220 When running coproID with the ancient DNA mode (`--adna`), alignments are filtered by PMDtools
221 (Skoglund et al., 2014) to only retain reads showing post-mortem damages (PMD). PMDtools default
222 settings are used, with specified library type, and only reads with a PMDScore greater than three are kept.

223 **Computing host DNA content**

224 Next, filtered alignments are processed in Python using the Pysam library (pysam developers, 2018).
225 Reads matching above the identity threshold of 0.95 to multiple host genomes are flagged as common
226 reads $reads_{commons}$ whereas reads mapping above the identity threshold to a single host genome are
227 flagged as genome-specific host reads $reads_{spec\ g}$ to each genome g . Each source species host DNA is
228 normalized by genome size and gut microbiome host DNA content such as:

$$229 \text{NormalizedHostDNA}(\text{source species}) = \frac{\sum \text{length}(reads_{spec\ g})}{genome_g \text{ length} \cdot endo_g} \quad (1)$$

230 where for each species of genome g , $\sum \text{length}(reads_{spec\ g})$ is the total length of all $reads_{spec\ g}$,
231 $genome_g \text{ length}$ is the size of the genome, and $endo_g$ is the host DNA proportion in the species gut
232 microbiome.

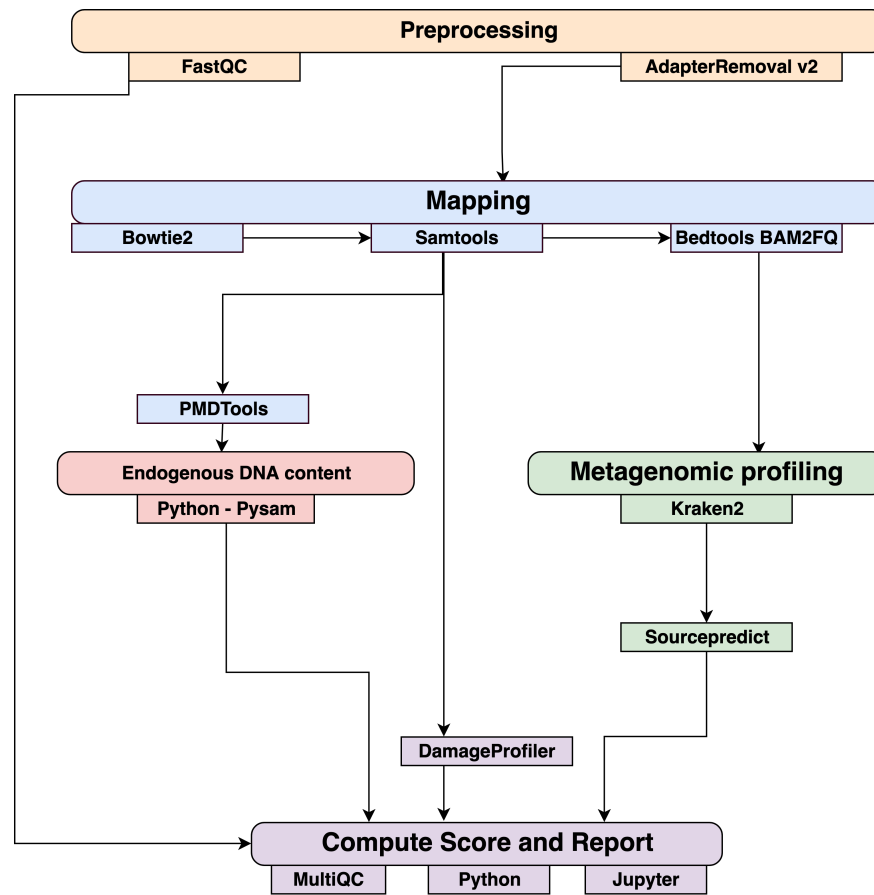


Figure 2. Workflow schematic of the coproID pipeline.

coproID consists of five steps: *Preprocessing* (orange), *Mapping* (blue), *Computing host DNA content for each metagenome* (red), *Metagenomic profiling* (green), and *Reporting* (violet). Individual programs (squared boxes) are colored by category (rounded boxes)

232 Afterwards, an host DNA ratio is computed for each source species such as:

$$233 \quad \text{NormalizedRatio}(\text{source species}) = \frac{\text{NormalizedHostDNA}(\text{source species})}{\sum \text{NormalizedHost DNA}(\text{source species})} \quad (2)$$

233 where $\sum \text{NormalizedHost DNA}(\text{source species})$ is the sum of all source species Normalized Host
234 DNA.

235 **Metagenomic profiling**

236 Adapter clipped and trimmed reads are given as an input to Kraken 2 (Wood and Salzberg, 2014). Using
237 the MiniKraken2_v2_8GB database (2019/04/23 version), Kraken 2 performs the taxonomic classification
238 to output a taxon count per sample report file. All samples taxon count are pooled together in a taxon
239 counts matrix with samples in columns, and taxons in rows. Next, Sourcepredict (Borry, 2019b) is used
240 to predict the source based on each microbiome sample taxon composition. Using dimension reduction and
241 K-Nearest Neighbors (KNN) machine learning trained with reference modern gut microbiomes samples
242 (Table 1), Sourcepredict estimates a proportion $\text{prop}_{\text{microbiome}}(\text{source species})$ of each potential source
243 species, here Human or Dog, for each sample.

244 **Reporting**

For each filtered alignment file, the DNA damage patterns are estimated with DamageProfiler (Peltzer and Neukamm, 2019). The information from the host DNA content and the metagenomic profiling are

gathered for each source in each sample such as:

$$proportion(source\ species) = NormalizedRatio(source\ species) \cdot prop_{microbiome}(source\ species)$$

245 Finally, a summary report is generated including the damage plots, a summary table of the coproID
246 metrics, and the embedding of the samples in two dimensions by Sourcepredict. coproID is available on
247 GitHub at the following address: github.com/nf-core/coproID.

248 RESULTS

249 We analyzed 21 archaeological samples with coproID v1.0 to estimate their source using both host DNA
250 and microbiome composition.

251 Host DNA in reference gut microbiomes

252 Before analyzing the archaeological samples, we first tested whether there is a per-species difference in
253 host DNA content in modern reference human and dog feces. With Anonymap, we computed the amount
254 of host DNA in each reference gut microbiome (Table S1). We found that the median percentages of
255 host DNA in NWHR, WHU, and Dog (Figure 3) are significantly different at $\alpha = 0.05$ (Kruskal-
256 Wallis H-test = 117.40, p value < 0.0001). We confirmed that there is a significant difference of median
257 percentages of host DNA between dogs and NWHR, as well as dogs and WHU, with Mann-Whitney U
258 tests (Table 3) and therefore corrected each sample by the mean percentage of gut host DNA found in
259 each species, 1.24% for humans ($\mu_{NWHR} = 0.85$, $\sigma_{NWHR} = 2.33$, $\mu_{WHU} = 1.67$, $\sigma_{WHU} = 0.81$), and 0.11%
260 for dogs ($\sigma_{dog} = 0.16$) (equation 1, table S1). This information was used to correct for the amount of host
261 DNA found in paleofeces.

Comparison	Mann–Whitney U test	p value
Dog vs NWHR	3327.0	< 0.0001
Dog vs WHU	41.0	< 0.0001
NWHR vs WHU	370.0	< 0.0001
Dog vs Human	3368.0	< 0.0001

Table 3. Statistical comparison of reference gut host DNA content. Mann–Whitney U test for independent observations. H_0 : the distributions of both populations are equal.

262 The effect of PMD filtering on host species prediction

263 Because aDNA accumulates damage over time (Briggs et al., 2007), we could use this characteristic to
264 filter for reads carrying these specific damage patterns using PMDtools, and therefore reduce modern
265 contamination in the dataset. We applied PMD filtering to our archaeological datasets, and for each,
266 compared the predicted host source before and afterwards. The predicted host sources did not change after
267 the DNA damage read filtering, but some became less certain (Figure 4). Most samples are confidently
268 assigned to one of the two target species, however some samples previously categorized as humans now lie
269 in the uncertainty zone. This suggests that PMDtools filtering lowered the modern human contamination
270 which might have originated from sample excavation and manipulation.

271 The trade-off of PMDtools filtering is that it reduces the assignment power by lowering the number
272 of reads available for host DNA based source prediction by only keeping PMD-bearing reads. This
273 loss is greater for well-preserved samples, which may have relatively few damaged reads (< 15% of
274 total). Ultimately, applying damage filtering can make it more difficult to categorize samples on the sole
275 basis of host DNA content, but it also makes source assignments more reliable by removing modern
276 contamination.

277 Source microbiome prediction of reference samples by Sourcepredict

278 To help resolve ambiguities related to the host aDNA present within a sample, we also investigated gut
279 microbiome composition as an additional line of evidence to better predict paleofeces source. After
280 performing taxonomic classification using Kraken2, we computed a sample pairwise distance matrix from
281 the species counts. With the t-SNE dimension reduction method, we embedded this distance matrix in

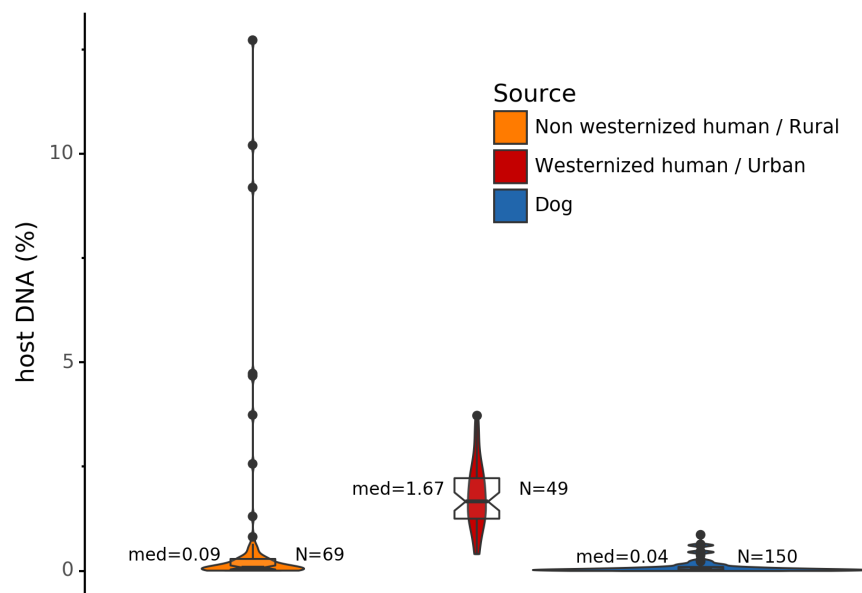


Figure 3. Gut microbiome host DNA content.

The median percentage of host DNA in the gut microbiome and the number of samples in each group are displayed besides each boxplot.

282 two dimensions to visualize the sample positions and sources (Figure 5a). We then used a KNN machine
283 learning classifier on this low dimension embedding to predict the source of gut microbiome samples.
284 This trained KNN model reached a test accuracy of 0.94 on previously unseen data (figure 5b).

285 **Embedding of archaeological samples by Sourcepredict**

286 We used this trained KNN model to predict the sources of the 20 paleofeces and coprolite archaeological
287 samples, after embedding them in a two-dimensional space (Figure 6). Based on their microbiome
288 composition data, Sourcepredict predicted 2 paleofeces samples as dogs, 8 paleofeces samples as human,
289 2 paleofeces samples and 4 archaeological sediments as soil, while the rest were predicted as unknown
290 (Table S2).

291 **coproID prediction**

292 Combining both PMD-filtered host DNA information and microbiome composition, coproID was able
293 to reliably categorize 7 of the 13 paleofeces samples, as 5 human paleofeces and 2 canine paleofeces,
294 whereas all of the non-fecal archaeological sediments were flagged as unknown. (Figure 8). This
295 confirms the original archaeological source hypothesis for five samples (ZSM005, ZSM025, ZSM027,
296 ZSM028, ZSM031) and specifies or rejects the original archaeological source hypothesis for the two
297 others (YRK001, AHP004). The 6 paleofeces samples not reliably identified by coproID have a conflicting
298 source proportion estimation between host DNA and microbiome composition (Figure 7a and 7b and
299 Table S3). Specifically, paleofeces AHP001, AHP002, and AHP003 show little predicted gut microbiome
300 preservation, and thus have likely been altered by taphonomic (decomposition) processes. Paleofeces
301 ZSM002, ZSM023, and ZSM029, by contrast, show good evidence of both host and microbiome
302 preservation, but have conflicting source predictions based on host and microbiome evidence. Given that
303 subsistence is associated with gut microbiome composition, this conflict may be related to insufficient gut
304 microbiome datasets available for non-Westernized dog populations (Hagan et al., 2019).

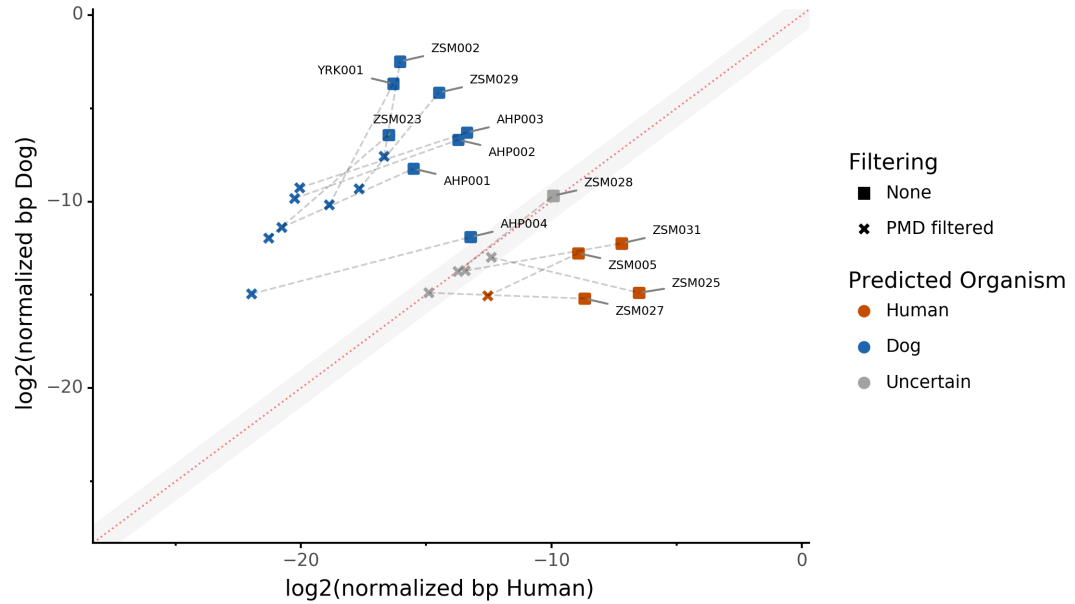


Figure 4. The effect of filtering for damaged reads using PMD.

The \log_2 of the human *NormalizedHostDNA* is graphed against the \log_2 of the dog *NormalizedHostDNA*. Squares represent samples before filtering by PMD, whereas crosses represent samples after filtering by PMD. Dotted lines show the correspondence between samples. The red diagonal line marks the boundary between the two species, and the grey shaded area indicates a zone of species uncertainty ($\pm 1 \log_2FC$) due to insufficient genetic information.

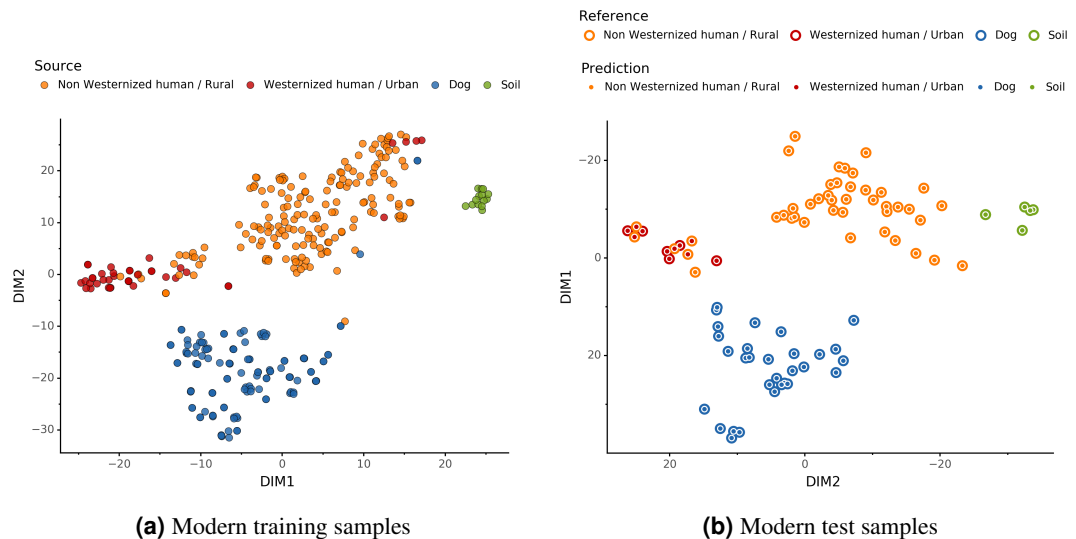


Figure 5. Embedding of reference modern gut microbiomes.

(a) t-SNE embedding of the species composition based on sample pairwise Weighted Unifrac distances for training modern gut microbiomes training samples. Samples are colored by their actual source. (b) t-SNE embedding of the species composition based on sample pairwise Weighted Unifrac distances for source prediction of modern test samples. The outer circle color is the actual source of a sample, while the inner circle color is the predicted sample source by Sourcepredict.

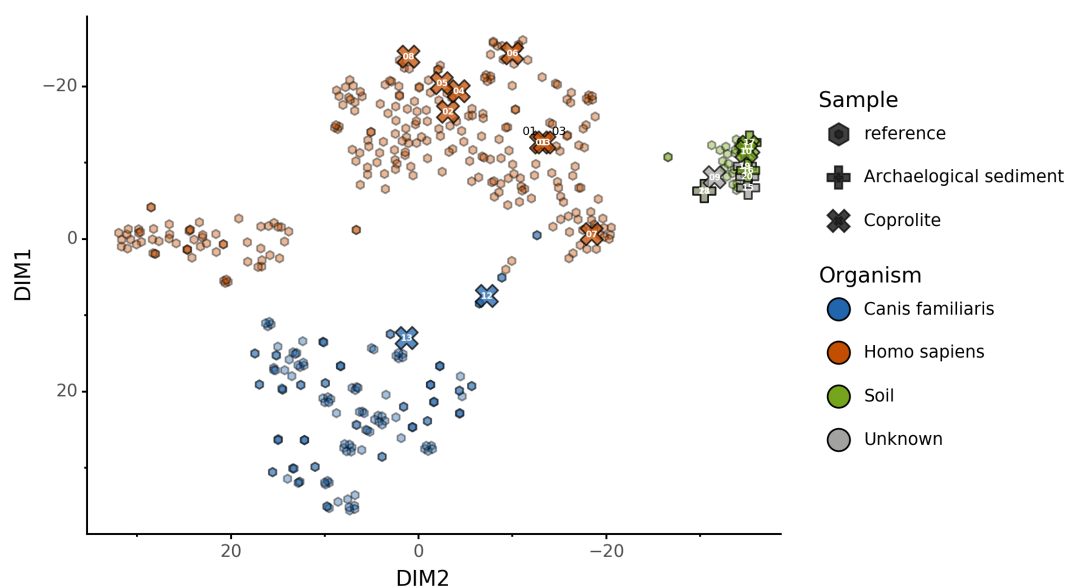


Figure 6. Prediction of archaeological samples sources and t-SNE embedding by Sourcepredict. t-SNE embedding of archaeological (crosses) and modern (hexagons) samples. The color of the modern samples is based on their actual source while the color of the archaeological samples is based on their predicted source by Sourcepredict. Archaeological sample are labelled with their *Plot ID* (Table 2).

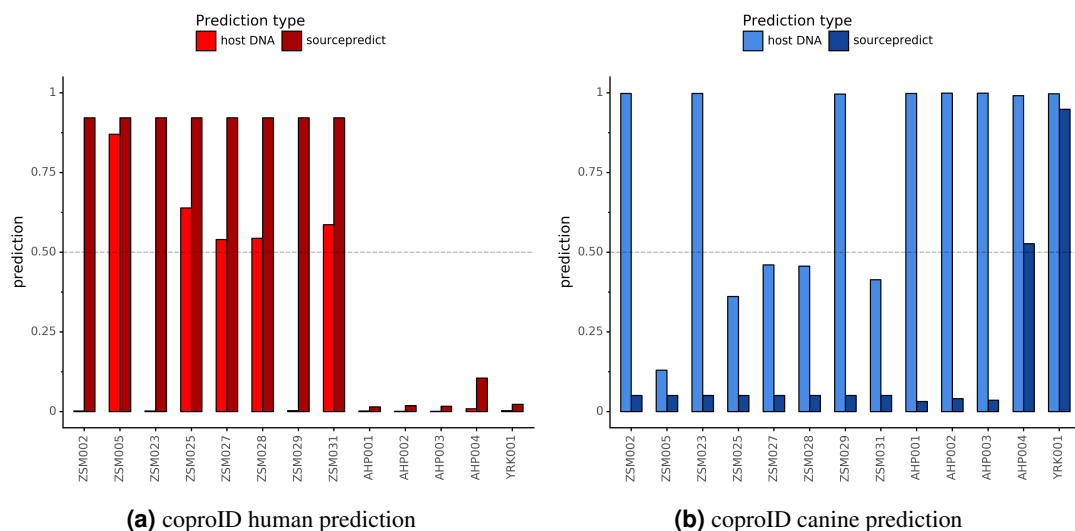


Figure 7. Host DNA and Sourcepredict source prediction for paleofeces samples. The vertical bar represents the predicted proportion by host DNA (lighter fill) or by Sourcepredict (darker fill). The horizontal dashed line represents the confidence threshold to assign a source to a sample.

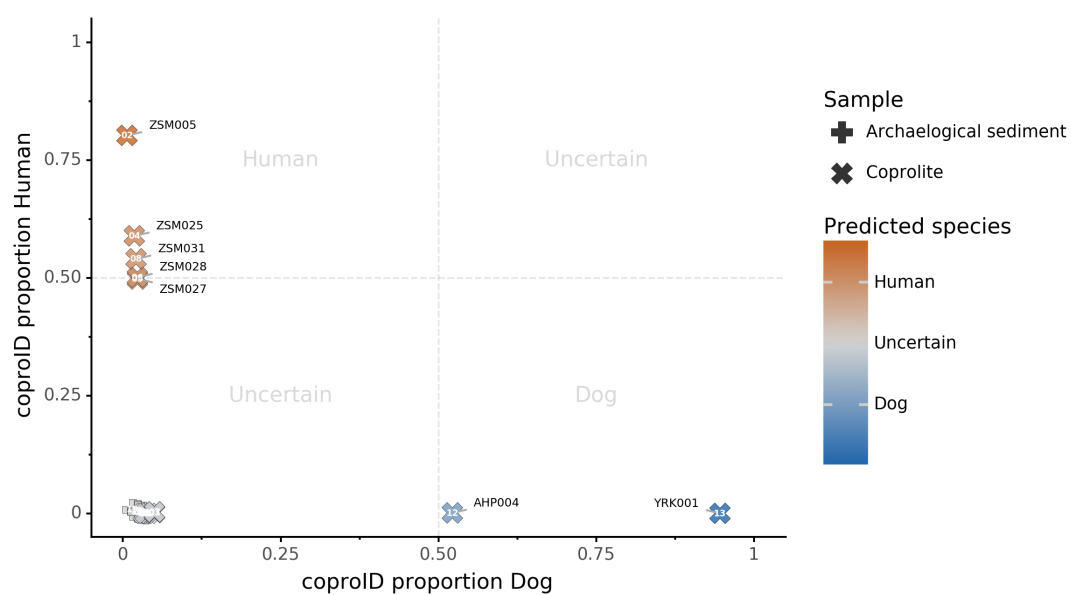


Figure 8. coproID source prediction.

Predicted human proportion graphed versus predicted canine proportion. Samples are colored by their predicted sources proportions. Samples with a low canine and human proportion are not annotated.

305 DISCUSSION

306 Paleofeces are the preserved remains of human or animal feces, and although they typically only preserve
307 under highly particular conditions, they are nevertheless widely reported in the paleontological and
308 archaeological records and include specimens ranging in age from the Paleozoic era (Dentzien-Dias et al.,
309 2013) to the last few centuries. Paleofeces can provide unprecedented insights into animal health and
310 diet, parasite biology and evolution, and the changing ecology and evolution of the gut microbiome.
311 However, because many paleofeces lack distinctive morphological features, determining the host origin of
312 a paleofeces can be a difficult problem (Poinar et al., 2009). In particular, distinguishing human and canine
313 paleofeces can be challenging because they are often similar in size and shape, they tend to co-occur
314 at archaeological sites and in midden deposits, and humans and domesticated dogs tend to eat similar
315 diets (Guiry, 2012). We developed coproID to aid in identifying the source organism of archaeological
316 paleofeces and coprolites by applying a combined approach relying on both ancient host DNA content
317 and gut microbiome composition.

318 coproID addresses several shortcomings of previous methods. First, we have included a DNA damage-
319 filtering step that allows for the removal of potentially contaminating modern human DNA, which may
320 otherwise skew host species assignment. We have additionally measured and accounted for significant
321 differences in the mean proportion of host DNA found in dog and human feces, and we also accounted for
322 differences in host genome size between humans and dogs when making quantitative comparisons of host
323 DNA. Then, because animal DNA recovered from paleofeces may contain a mixture of host and dietary
324 DNA, we also utilize gut microbiome compositional data to estimate host source. We show that humans
325 and dogs have distinct gut microbiome compositions, and that their feces can be accurately distinguished
326 from each other and from non-feces using a machine learning classifier after data dimensionality reduction.
327 Taken together, these approaches allow a robust determination of paleofeces and coprolite host source, that
328 takes into account both modern contamination, microbiome composition, and postmortem degradation.

329 In applying coproID to a set of 20 archaeological samples of known and/or suspected origin, all
330 7 non-fecal sediment samples were accurately classified as "uncertain" and were grouped with soil
331 by Sourcepredict. For the 13 paleofeces and coprolites under study, 7 exhibited matching host and
332 microbiome source assignments and were confidently classified as either human (n=5) or canine (n=2).
333 Importantly, one of the samples confidently identified as canine was YRK001, a paleofeces that had been
334 recovered from an archaeological chamber pot in the United Kingdom, but which showed an unusual
335 diversity of parasites inconsistent with human feces, and therefore posed issues in host assignment.

336 For the remaining six unidentified paleofeces, three exhibited poor microbiome preservation and were
337 classified as "uncertain", while the other three were well-preserved but yielded conflicting host DNA
338 and microbiome assignments. These three samples, ZSM002, Z023, and ZSM029, all from prehistoric
339 Mexico, all contain high levels of canine DNA, but have gut microbiome profiles within the range of
340 NWHR humans. Classified as "uncertain", there are two possible explanations for these samples. First,
341 these feces could have originated from a human who consumed a recent meal of canine meat. Dogs
342 were consumed in ancient Mesoamerica (Clutton-Brock and Hammond, 1994; Santley and Rose, 1979;
343 Rosenswig, 2007; Wing, 1978), but further research on the expected proportion of dietary DNA in human
344 feces is needed to determine whether this is a plausible explanation for the very high amounts of canine
345 DNA (and negligible amounts of human DNA) observed.

346 Alternatively, these feces could have originated from a canine whose microbiome composition is
347 shifted relative to that of the reference metagenomes used in our training set. It is now well-established
348 that subsistence mode strongly influences gut microbiome composition in humans Obregon-Tito et al.
349 (2015), with NWHR and WHU human populations largely exhibiting distinct gut microbiome structure,
350 as seen in (Figure 5a. To date, no gut microbiome data is available from non-Westernized dogs, and all
351 reference dog metagenome data included as training data for coproID originated from a single study of
352 labrador retrievers and beagles Coelho et al. (2018). Future studies of non-Westernized rural dogs are
353 needed to establish the full range of gut microbial diversity in dogs and to more accurately model dog gut
354 microbiome diversity in the past. Given that all confirmed human paleofeces in this study falls within
355 the NWHR cluster (Figure 6), we anticipate that our ability to accurately classify dog paleofeces and
356 coprolites as canine (as opposed to "uncertain") will improve with the future addition of non-Westernized
357 rural dog metagenomic data.

358 CONCLUSIONS

359 We developed an open-source, documented, tested, scalable, and reproducible method to perform the
360 identification of archaeological paleofeces and coprolite source. By leveraging the information from
361 host DNA and microbiome composition, we were able to identify and/or confirm the source of newly
362 sequenced paleofeces. We demonstrated that coproID can provide useful assistance to archaeologists in
363 identifying authentic paleofeces and inferring their host. Future work on dog gut microbiome diversity,
364 especially among rural, non-Westernized dogs, may help improve the tool's sensitivity even further.

365 ACKNOWLEDGMENTS

366 We thank David Petts, Zdeněk Tvrdý, Susanne Stegmann-Rajtár, and Zuzana Rajtarova for contributing
367 archaeological samples to this study. We thank the Guildford Museum (Guildford Borough Council
368 Heritage Service) and Catriona Wilson for allowing us to analyze the chamber pot paleofeces sample from
369 Surrey, UK. The sample from Derragh, Ireland was excavated by Discovery Programme, an all-Ireland
370 public center of archaeological research supported by the Heritage Council, during field work in 2003 to
371 2005 as part of the Lake Settlement Project. Thanks to the Servei d'Investigació Prehistòrica of València
372 and Museu de la Valltorta of Catelló for access to material. This work was supported by the US National
373 Institutes of Health R01GM089886 (to C.W. and C.M.L.), the Deutsche Forschungsgemeinschaft EXC
374 2051 #390713860 (to C.W.), and the Max Planck Society. Author contributions were as follows: M.B.
375 and C.W. designed the research. B.C., M.C.W., D.J., C.A.H., and R.W.H. performed the laboratory
376 experiments. M.B., C.J., M.C.W. and T.H. analyzed the data. M.B. developed the bioinformatics tools
377 and pipelines. C.W., K.R., K.B., L.G.F., A.P., A.K., W.T.J.K., R.P., I.S., D.S.G., J.Y., T.S.K., N.M., H.C.,
378 and C.M.L. provided materials and resources. C.W., A.He., and A.Hü. supervised the research. M.B.
379 wrote the article, with input from C.W., A.Hü., KR and the other co-authors.

380 DATA AND CODE AVAILABILITY

381 Genetic data are available in the European Nucleotide Archive (ENA) under the accessions PRJEB33577
382 and PRJEB35362. The code for the analysis is available at github.com/maxibor/coproid-article.

383 REFERENCES

- 384 Andrews, S. et al. (2010). Fastqc: a quality control tool for high throughput sequence data.
385 Bon, C., Berthonaud, V., Maksud, F., Labadie, K., Poulain, J., Artiguenave, F., Wincker, P., Aury, J.-M.,
386 and Elalouf, J.-M. (2012). Coprolites as a source of information on the genome and diet of the cave
387 hyena. *Proceedings of the Royal Society B: Biological Sciences*, 279(1739):2825–2830.
388 Borry, M. (2019a). maxibor/anonymap: Anonymap v1.0.
389 Borry, M. (2019b). Sourcepredict: Prediction of metagenomic sample sources using dimension reduction
390 followed by machine learning classification. *Journal of Open Source Software*, 4(41):1540.
391 Briggs, A. W., Stenzel, U., Johnson, P. L. F., Green, R. E., Kelso, J., Prüfer, K., Meyer, M., Krause, J.,
392 Ronan, M. T., Lachmann, M., and Pääbo, S. (2007). Patterns of damage in genomic DNA sequences
393 from a Neandertal. *Proceedings of the National Academy of Sciences*, 104(37):14616–14621.
394 Brito, I. L., Gurry, T., Zhao, S., Huang, K., Young, S. K., Shea, T. P., Naisilisili, W., Jenkins, A. P., Jupiter,
395 S. D., Gevers, D., and Alm, E. J. (2019). Transmission of human-associated microbiota along family
396 and social networks. *Nature Microbiology*, page 1.
397 Butler, J. and Du Toit, J. (2002). Diet of free-ranging domestic dogs (*canis familiaris*) in rural zimbabwe:
398 implications for wild scavengers on the periphery of wildlife reserves. In *Animal Conservation forum*,
399 volume 5, pages 29–37. Cambridge University Press.
400 Clutton-Brock, J. and Hammond, N. (1994). Hot dogs: comestible canids in preclassic maya culture at
401 cuello, belize. *Journal of Archaeological Science*, 21(6):819–826.
402 Coelho, L. P., Kultima, J. R., Costea, P. I., Fournier, C., Pan, Y., Czarnecki-Maulden, G., Hayward, M. R.,
403 Forslund, S. K., Schmidt, T. S. B., Descombes, P., Jackson, J. R., Li, Q., and Bork, P. (2018). Similarity
404 of the dog and human gut microbiomes in gene content and response to diet. *Microbiome*, 6(1):72.
405 CSIR, C. i. o. m. and aromatic plants (2016). *Chrysopogon zizanioides* (ID 322597) - BioProject - NCBI.
406 Dabney, J., Knapp, M., Glocke, I., Gansauge, M.-T., Weihmann, A., Nickel, B., Valdiosera, C., García,
407 N., Pääbo, S., Arsuaga, J.-L., et al. (2013). Complete mitochondrial genome sequence of a middle

- 408 pleistocene cave bear reconstructed from ultrashort dna fragments. *Proceedings of the National*
409 *Academy of Sciences*, 110(39):15758–15763.
- 410 Davenport, E. R., Sanders, J. G., Song, S. J., Amato, K. R., Clark, A. G., and Knight, R. (2017). The
411 human microbiome in evolution. *BMC Biology*, 15(1):127.
- 412 Dentzien-Dias, P. C., Poinar Jr, G., de Figueiredo, A. E. Q., Pacheco, A. C. L., Horn, B. L., and Schultz,
413 C. L. (2013). Tapeworm eggs in a 270 million-year-old shark coprolite. *PLoS One*, 8(1):e55007.
- 414 Dhakan, D. B., Maji, A., Sharma, A. K., Saxena, R., Pulikkan, J., Grace, T., Gomez, A., Scaria, J., Amato,
415 K. R., and Sharma, V. K. (2019). The unique composition of Indian gut microbiome, gene catalogue,
416 and associated fecal metabolome deciphered using multi-omics approaches. *GigaScience*, 8(3).
- 417 Di Tommaso, P., Chatzou, M., Floden, E. W., Barja, P. P., Palumbo, E., and Notredame, C. (2017).
418 Nextflow enables reproducible computational workflows. *Nature biotechnology*, 35(4):316.
- 419 Ewels, P., Peltzer, A., Fillinger, S., Alneberg, J., Patel, H., Wilm, A., Garcia, M., Di Tommaso, P., and
420 Nahnsen, S. (2019). nf-core: Community curated bioinformatics pipelines. *bioRxiv*, page 610741.
- 421 Fierer, N., Leff, J. W., Adams, B. J., Nielsen, U. N., Bates, S. T., Lauber, C. L., Owens, S., Gilbert,
422 J. A., Wall, D. H., and Caporaso, J. G. (2012). Cross-biome metagenomic analyses of soil micro-
423 bial communities and their functional attributes. *Proceedings of the National Academy of Sciences*,
424 109(52):21390–21395.
- 425 Frantz, L. A., Mullin, V. E., Pionnier-Capitan, M., Lebrasseur, O., Ollivier, M., Perri, A., Linderholm,
426 A., Mattiangeli, V., Teasdale, M. D., Dimopoulos, E. A., et al. (2016). Genomic and archaeological
427 evidence suggest a dual origin of domestic dogs. *Science*, 352(6290):1228–1231.
- 428 Gilbert, M. T. P., Jenkins, D. L., Götherstrom, A., Naveran, N., Sanchez, J. J., Hofreiter, M., Thomsen,
429 P. F., Binladen, J., Higham, T. F., Yohe, R. M., et al. (2008). Dna from pre-clovis human coprolites in
430 oregon, north america. *Science*, 320(5877):786–789.
- 431 Guiry, E. J. (2012). Dogs as analogs in stable isotope-based human paleodietary reconstructions: a review
432 and considerations for future use. *Journal of Archaeological Method and Theory*, 19(3):351–376.
- 433 Hagan, R. W., Hofman, C. A., Hübner, A., Reinhard, K., Schnorr, S., Lewis, C. M., Sankaranarayanan,
434 K., and Warinner, C. G. (2019). Comparison of extraction methods for recovering ancient microbial
435 dna from paleofeces. *American Journal of Physical Anthropology*.
- 436 Hofreiter, M., Poinar, H. N., Spaulding, W. G., Bauer, K., Martin, P. S., Possnert, G., and Pääbo, S.
437 (2000). A molecular analysis of ground sloth diet through the last glaciation. *Molecular Ecology*,
438 9(12):1975–1984.
- 439 Huttenhower, C., Gevers, D., Knight, R., Abubucker, S., Badger, J. H., Chinwalla, A. T., Creasy, H. H.,
440 Earl, A. M., FitzGerald, M. G., Fulton, R. S., et al. (2012). Structure, function and diversity of the
441 healthy human microbiome. *nature*, 486(7402):207.
- 442 Jiménez, F. A., Gardner, S. L., Araújo, A., Fugassa, M., Brooks, R. H., Racz, E., and Reinhard, K. J.
443 (2012). Zoonotic and human parasites of inhabitants of cueva de los muertos chiquitos, rio zape valley,
444 durango, mexico. *Journal of Parasitology*, 98(2):304–310.
- 445 Kho, Z. Y. and Lal, S. K. (2018). The human gut microbiome—a potential controller of wellness and
446 disease. *Frontiers in microbiology*, 9.
- 447 Kirch, P. and O’Day, S. J. (2003). New archaeological insights into food and status: a case study from
448 pre-contact hawaii. *World Archaeology*, 34(3):484–497.
- 449 Knights, D., Kuczynski, J., Charlson, E. S., Zaneveld, J., Mozer, M. C., Collman, R. G., Bushman, F. D.,
450 Knight, R., and Kelley, S. T. (2011). Bayesian community-wide culture-independent microbial source
451 tracking. *Nature Methods*, 8(9):761–763.
- 452 Langmead, B. and Salzberg, S. L. (2012). Fast gapped-read alignment with bowtie 2. *Nature methods*,
453 9(4):357.
- 454 Ley, R. E., Hamady, M., Lozupone, C., Turnbaugh, P. J., Ramey, R. R., Bircher, J. S., Schlegel, M. L.,
455 Tucker, T. A., Schrenzel, M. D., Knight, R., et al. (2008). Evolution of mammals and their gut microbes.
456 *Science*, 320(5883):1647–1651.
- 457 Mann, A. E., Sabin, S., Ziesemer, K., Vågane, Å. J., Schroeder, H., Ozga, A. T., Sankaranarayanan,
458 K., Hofman, C. A., Yates, J. A. F., Salazar-García, D. C., et al. (2018). Differential preservation of
459 endogenous human and microbial dna in dental calculus and dentin. *Scientific reports*, 8(1):9822.
- 460 Meyer, M. and Kircher, M. (2010). Illumina sequencing library preparation for highly multiplexed target
461 capture and sequencing. *Cold Spring Harbor Protocols*, 2010(6):pdb-prot5448.
- 462 Obregon-Tito, A. J., Tito, R. Y., Metcalf, J., Sankaranarayanan, K., Clemente, J. C., Ursell, L. K.,

- 463 Zech Xu, Z., Van Treuren, W., Knight, R., Gaffney, P. M., Spicer, P., Lawson, P., Marin-Reyes, L.,
464 Trujillo-Villarroel, O., Foster, M., Guija-Poma, E., Troncoso-Corzo, L., Warinner, C., Ozga, A. T., and
465 Lewis, C. M. (2015). Subsistence strategies in traditional societies distinguish gut microbiomes. *Nature*
466 *Communications*, 6:6505.
- 467 Orellana, L. H., Chee-Sanford, J. C., Sanford, R. A., Löffler, F. E., and Konstantinidis, K. T. (2018).
468 Year-Round Shotgun Metagenomes Reveal Stable Microbial Communities in Agricultural Soils and
469 Novel Ammonia Oxidizers Responding to Fertilization. *Applied and Environmental Microbiology*,
470 84(2):e01646–17.
- 471 Pasolli, E., Asnicar, F., Manara, S., Zolfo, M., Karcher, N., Armanini, F., Beghini, F., Manghi, P., Tett,
472 A., Ghensi, P., Collado, M. C., Rice, B. L., DuLong, C., Morgan, X. C., Golden, C. D., Quince,
473 C., Huttenhower, C., and Segata, N. (2019). Extensive Unexplored Human Microbiome Diversity
474 Revealed by Over 150,000 Genomes from Metagenomes Spanning Age, Geography, and Lifestyle.
475 *Cell*, 176(3):649–662.e20.
- 476 Peltzer, A. and Neukamm, J. (2019). Integrative-Transcriptomics/DamageProfiler: DamageProfiler v0.4.7.
- 477 Podberscek, A. L. (2009). Good to pet and eat: The keeping and consuming of dogs and cats in south
478 korea. *Journal of Social Issues*, 65(3):615–632.
- 479 Poinar, H., Fiedel, S., King, C. E., Devault, A. M., Bos, K., Kuch, M., and Debruyne, R. (2009). Comment
480 on “dna from pre-clovis human coprolites in oregon, north america”. *Science*, 325(5937):148–148.
- 481 Poinar, H. N., Hofreiter, M., Spaulding, W. G., Martin, P. S., Stankiewicz, B. A., Bland, H., Evershed,
482 R. P., Possnert, G., and Pääbo, S. (1998). Molecular coproscopy: dung and diet of the extinct ground
483 sloth *nothrotheriops shastensis*. *Science*, 281(5375):402–406.
- 484 Poinar, H. N., Kuch, M., Sobolik, K. D., Barnes, I., Stankiewicz, A. B., Kuder, T., Spaulding, W. G.,
485 Bryant, V. M., Cooper, A., and Pääbo, S. (2001). A molecular analysis of dietary diversity for three
486 archaic native americans. *Proceedings of the National Academy of Sciences*, 98(8):4317–4322.
- 487 pysam developers (2018). Pysam: a python module for reading and manipulating files in the sam/bam
488 format.
- 489 Rampelli, S., Schnorr, S., Consolandi, C., Turroni, S., Severgnini, M., Peano, C., Brigidi, P., Crittenden,
490 A., Henry, A., and Candela, M. (2015). Metagenome Sequencing of the Hadza Hunter-Gatherer Gut
491 Microbiota. *Current Biology*, 25(13):1682–1693.
- 492 Rohland, N., Harney, E., Mallick, S., Nordenfelt, S., and Reich, D. (2015). Partial uracil–dna–glycosylase
493 treatment for screening of ancient dna. *Philosophical Transactions of the Royal Society B: Biological*
494 *Sciences*, 370(1660):20130624.
- 495 Rosenswig, R. M. (2007). Beyond identifying elites: Feasting as a means to understand early middle
496 formative society on the pacific coast of mexico. *Journal of Anthropological Archaeology*, 26(1):1–27.
- 497 Santley, R. S. and Rose, E. K. (1979). Diet, nutrition and population dynamics in the basin of mexico.
498 *World Archaeology*, 11(2):185–207.
- 499 Schubert, M., Lindgreen, S., and Orlando, L. (2016). Adapterremoval v2: rapid adapter trimming,
500 identification, and read merging. *BMC research notes*, 9(1):88.
- 501 Sharpton, T. J. (2014). An introduction to the analysis of shotgun metagenomic data. *Frontiers in plant*
502 *science*, 5:209.
- 503 Shenhav, L., Thompson, M., Joseph, T. A., Briscoe, L., Furman, O., Bogumil, D., Mizrahi, I., Pe’er, I.,
504 and Halperin, E. (2019). FEAST: fast expectation-maximization for microbial source tracking. *Nature*
505 *Methods*, page 1.
- 506 Sistiaga, A., Mallol, C., Galván, B., and Summons, R. E. (2014). The neanderthal meal: a new perspective
507 using faecal biomarkers. *PLoS one*, 9(6):e101045.
- 508 Skoglund, P., Northoff, B. H., Shunkov, M. V., Derevianko, A. P., Pääbo, S., Krause, J., and Jakobsson, M.
509 (2014). Separating endogenous ancient DNA from modern day contamination in a Siberian Neandertal.
510 *Proceedings of the National Academy of Sciences*, 111(6):2229–2234.
- 511 The Human Microbiome Project Consortium, Huttenhower, C., Gevers, D., Knight, Rob, W. O., et al.
512 (2012). Structure, function and diversity of the healthy human microbiome. *Nature*, 486(7402):207–214.
- 513 Tito, R. Y., Knights, D., Metcalf, J., Obregon-Tito, A. J., Cleeland, L., Najar, F., Roe, B., Reinhard, K.,
514 Sobolik, K., Belknap, S., Foster, M., Spicer, P., Knight, R., and Lewis, C. M. (2012). Insights from
515 Characterizing Extinct Human Gut Microbiomes. *PLoS ONE*, 7(12):e51146.
- 516 Tito, R. Y., Macmil, S., Wiley, G., Najar, F., Cleeland, L., Qu, C., Wang, P., Romagne, F., Leonard, S.,
517 Ruiz, A. J., et al. (2008). Phylotyping and functional analysis of two ancient human microbiomes.

- 518 *PLoS One*, 3(11):e3703.
- 519 Warinner, C., Herbig, A., Mann, A., Fellows Yates, J. A., Weiß, C. L., Burbano, H. A., Orlando, L., and
520 Krause, J. (2017). A robust framework for microbial archaeology. *Annual review of genomics and*
521 *human genetics*, 18:321–356.
- 522 Warinner, C. and Lewis Jr, C. M. (2015). Microbiome and health in past and present human populations.
523 *American Anthropologist*, 117(4):740–741.
- 524 Warinner, C., Speller, C., Collins, M. J., and Lewis Jr, C. M. (2015). Ancient human microbiomes.
525 *Journal of human evolution*, 79:125–136.
- 526 Wing, E. S. (1978). *Use of dogs for food: An adaptation to the coastal environment*. Elsevier.
- 527 Wood, D. E. and Salzberg, S. L. (2014). Kraken: ultrafast metagenomic sequence classification using
528 exact alignments. *Genome biology*, 15(3):R46.
- 529 Wood, J. R., Crown, A., Cole, T. L., and Wilmshurst, J. M. (2016). Microscopic and ancient dna profiling
530 of polynesian dog (kuri) coprolites from northern new zealand. *Journal of Archaeological Science:*
531 *Reports*, 6:496–505.